

Silver-nanoparticle-assisted photocurrent generation in polythiophene-fullerene thin films

You, Jing

Department of Materials Physics and Chemistry, Graduate School of Engineering, Kyushu University

Arakawa, Taichi

Department of Materials Physics and Chemistry, Graduate School of Engineering, Kyushu University

Munaoka, Takatoshi

Department of Materials Physics and Chemistry, Graduate School of Engineering, Kyushu University

Akiyama, Tsuyoshi

Department of Materials Science, School of Engineering, The University of Shiga Prefecture |
Department of Materials Physics and Chemistry, Graduate School of Engineering, Kyushu University

他

<https://hdl.handle.net/2324/25592>

出版情報 : Japanese Journal of Applied Physics. 50 (4 PART 2), pp.04DK22(1)-04DK22(4), 2011-04-20. The Japan Society of Applied Physics

バージョン :

権利関係 : (C) 2012 The Japan Society of Applied Physics



Silver-Nanoparticle-Assisted Photocurrent Generation in Polythiophene-Fullerene Thin Films

Jing You¹, Taichi Arakawa¹, Takatoshi Munaoka¹, Tsuyoshi Akiyama^{1,2,3}, Yukina Takahashi^{1,2}, and Sunao Yamada^{1,2*}

¹Department of Materials Physics and Chemistry, Graduate School of Engineering,
Kyushu University, Fukuoka 819-0395, Japan

²Department of Applied Chemistry, Faculty of Engineering,
Kyushu University, Fukuoka 819-0395, Japan

*E-mail address: yamada@mail.cstm.kyushu-u.ac.jp

³Department of Materials Science, School of Engineering,
The University of Shiga Prefecture, Hikone, Shiga 522-8583, Japan

* To whom correspondence should be addressed. E-mail address:
yamada@mail.cstm.kyushu-u.ac.jp

Abstract

We have investigated the effect of silver nanoparticles (AgPs) on the photocurrent generation of a polythiophene-fullerene photovoltaic film. Poly(3-hexylthiophene) (P3HT) and [6,6]-phenyl-C₆₁-butyric acid methylester (PCBM) were used for the electron donor and acceptor, respectively. First, AgPs were electrostatically deposited upon the surface of an indium tin oxide (ITO) electrode via a polycation. Then, a film of P3HT or a mixture of P3HT and PCBM was prepared by spin coating. The thickness of the film was evaluated by atomic force microscopy. Absorption and fluorescence spectral measurements were carried out to investigate the effects of AgPs. Photocurrent spectra were also measured, and the effects of AgPs on photocurrent enhancement were verified.

1. Introduction

Solar energy conversion is one of the promising approaches for creating clean energy systems. Recently, organic thin-film solar cells have attracted much attention from scientific and technical viewpoints toward the development of the next generation of solar cells.¹⁻⁴⁾ In particular, a polythiophene-fullerene thin film is used in bulk heterojunction solar cells as the photovoltaic layer. Poly(3-hexylthiophene) (P3HT) and [6,6]-phenyl-C₆₁-butyric acid methylester (PCBM), derivatives of polythiophene and fullerene, respectively (Fig. 1), are currently used to fabricate thin films in order to increase their solubility.⁴⁻⁷⁾

Figure 1

The process of photoelectric conversion in P3HT-PCBM film is as follows: the film absorbs incident photons and produces electron-hole pairs (excitons); then the pairs separate and charges are collected at electrodes. Compared with inorganic semiconductors, the charge mobilities of organic materials are much lower. In order to improve the charge mobility, organic films must be fabricated as thin as possible with sufficient photoabsorption.⁸⁾

When a nanosize metal particle is activated by light, the collective oscillation of conduction electrons occurs on the particle surface, which is called localized surface plasmon resonance (LSPR).⁹⁾ It exhibits unique phenomena such as intense absorption at a wavelength resonant with the electronic transition of molecules in the UV-vis region. LSPR is also used to enhance the absorption of silicon solar cells.¹⁰⁻¹³⁾ Moreover, the enhanced electric field adhering to the surface region of particles can be applied to enhance fluorescence intensity.¹⁴⁻¹⁶⁾ In dye-sensitized solar cells (DSSCs), LSPR has also been used to enhance the extinction of dyes.¹⁷⁾

Recently, LSPR has been widely used in solid-state photodiodes,¹⁸⁻²²⁾

photodetectors,²³⁻²⁵⁾ solar cells,²⁶⁻³⁰⁾ and so forth. There are many methods of fabricating metal nanoparticles on the surface of indium tin oxide (ITO) electrodes, such as vacuum deposition, lithography, casting from a colloidal solution, electrostatic layer-by-layer adsorption, and so forth.^{21-25, 27, 28, 31, 32)} Vacuum deposition and lithography have the disadvantages of sophisticated instrumentation, high cost, and difficulty in controlling the density and the size of nanoparticles.

In the present study, we used a simple method of immobilizing silver nanoparticles (AgPs) as reported before^{31, 32)} to fabricate a AgPs layer on the surface of ITO glass. The density of AgPs on the ITO surface was controlled by varying the immersion time. Then, P3HT-PCBM thin films on the surface of the AgPs layer were fabricated by spin-coating. We investigated the influence of the AgPs layer on the photocurrent and fluorescence of a P3HT layer with and without PCBM. Furthermore, we measured the size and surface morphology of AgPs layer by atomic force microscopy (AFM).

2. Experimental Procedure

All chemicals were commercially obtained and used as received. Silver nanoparticles were prepared as described previously³²⁾. The fabrication procedures of four types of film samples are illustrated in Fig. 2. The surface of the ITO electrode was cleaned by ultrasonication in ethanol and acetone, and then exposed to ozone for 30 min. Then, the ITO electrode was immersed into a solution of poly(ethylene imine) (PEI; 45 g/L in 1 M aq. NaCl) for 30 min at 30 °C, followed by washing with water and drying by nitrogen flow, giving a PEI-modified ITO electrode. The deposition of PEI was important to avoid the peeling off AgPs from the electrode surface. Next, the ITO electrode was immersed into an aqueous solution of AgPs for 10 h at 30 °C, followed by washing with

Figure 2

water and drying by nitrogen flow, resulting in the formation of a AgP layer on the ITO electrode, denoted as ITO/AgP.¹⁰⁾ Finally, a chlorobenzene solution of RR-P3HT (0.2 mg/mL) or of P3HT:PCBM (0.2 mg/mL each) was spin-coated on the surface of ITO/AgP, giving sample films of ITO/AgP/P3HT or ITO/AgP/P3HT:PCBM, respectively. As reference films, we fabricated ITO/P3HT and ITO/P3HT:PCBM by spin-coating the corresponding solution onto the ITO electrode.

Transmission absorption and fluorescence spectra were measured on JASCO V-670 and JASCO FP-6600 spectrophotometers, respectively. Photocurrent measurements were carried out using a standard three-electrode photoelectrochemical cell, where the film samples, Ag wire, and Ag/AgCl (saturated KCl solution) were used as working, counter, and reference electrodes, respectively. In the photocurrent measurements, an aqueous solution of 0.1 M NaClO₄ was used as the electrolyte solution. The excitation light from a Xe lamp propagated through a monochromator and irradiated the sample films. The photocurrent was measured by changing the excitation wavelength at the applied potential of 0 V vs Ag/AgCl (saturated KCl solution). In all samples, the photocurrent was observed in the cathodic direction.

3. Results and Discussion

In order to characterize the sample films, we carried out some spectroscopic measurements. Figure 3 shows transmission absorption spectra of ITO/AgP/P3HT, ITO/AgP/P3HT:PCBM, ITO/P3HT, and ITO/P3HT:PCBM. In ITO/AgP/P3HT and ITO/AgP/P3HT:PCBM films, broad bands around 420 nm based on the plasmon bands of AgPs can be seen with comparable intensities. Broad bands around 600-800 nm are

Figure 3

mainly due to the unavoidable interference effects of the incident light owing to the presence of AgPs. The broadening and redshift of the plasmon resonance by interparticle plasmon coupling among the AgPs must also be taken into consideration to some extent.^{32, 33)}

As has been reported previously, P3HT has strong absorption in the 450-650 nm region,³⁴⁾ while the absorption bands of PCBM appearing in the visible region^{35~37)} are small compared with the plasmon bands and absorption bands of P3HT. Thus, the bands of PCBM could not be identified in this study. The broad band in the 400-600 nm region for ITO/P3HT and ITO/P3HT:PCBM is clearly due to the absorption of P3HT. However, this band is not clear in ITO/AgP/P3HT or ITO/AgP/P3HT:PCBM. There seem to be two plausible reasons for this: one is the overlapping with the strong plasmon band of AgPs, and the other is the reduced thickness of films in the presence of AgPs (*vide infra*).

Figure 4

In order to clarify the morphology of the as-prepared films, AFM measurements were carried out. Figure 4 shows AFM images of AgPs deposited on the surface of ITO (ITO/AgP/P3HT and ITO/AgP/P3HT:PCBM). It is clear that ITO/AgP/P3HT and ITO/AgP/P3HT:PCBM have considerable amounts of AgPs with some aggregation. The thicknesses of P3HT or P3HT:PCBM for the sample films (see supporting information) were estimated to be 15 ± 5 nm for ITO/AgP/P3HT, 21 ± 3 nm for ITO/AgP/P3HT:PCBM, 25 ± 5 nm for ITO/P3HT, and 33 ± 6 nm for ITO/P3HT:PCBM. Consequently, the thicknesses of the P3HT layers are clearly different with and without AgPs. This must be caused by the change in the spreading property of the sample solution in the presence of AgPs on the ITO surface. From Fig. 4, we also estimated the mean size of AgPs, which was evaluated to be 71 nm (for

ITO/AgP/P3HT and ITO/AgP/P3HT), and the coverages of AgPs on the ITO surfaces were estimated to be 86 and 76%, respectively.

Figure 5 shows fluorescence spectra of ITO/AgP/P3HT, ITO/AgP/P3HT:PCBM, ITO/P3HT, and ITO/P3HT:PCBM, based on the fluorescence from the excited P3HT (excitation wavelength: 530 nm). In order to investigate the effect of PCBM, the fluorescence of ITO/AgP/P3HT and ITO/AgP/P3HT:PCBM and that of ITO/P3HT and ITO/P3HT:PCBM were compared. Clearly, the fluorescence was considerably reduced in the presence of PCBM, regardless of the presence or absence of AgPs. The effect of AgPs was investigated by comparing the fluorescence of ITO/AgP/P3HT and ITO/P3HT and that of ITO/AgP/P3HT:PCBM and ITO/P3HT:PCBM. It is clear that the presence of AgPs enhanced the fluorescence, even when taking into consideration the large difference in the thickness of organic layers. This means that efficient electron-transfer quenching from the excited P3HT to PCBM is realized in ITO/AgP/P3HT:PCBM and ITO/P3HT:PCBM. Thus, the enhancement of molecular excitation by the plasmon electric field as well as the scattering light is strongly indicated to occur in ITO/AgP/P3HT and ITO/AgP/P3HT:PCBM, as in the case of a porphyrin-AgP system.³²⁾

Figure 5

As has been reported previously,³⁷⁾ the photocurrent signal from the P3HT thin film increased smoothly with increasing thickness of the P3HT layer up to about 100 nm. The incident photon to current conversion efficiency (IPCE) values for P3HT and P3HT:PCBM films became considerably larger upon the addition of AgPs (compare ITO/AgP/P3HT vs ITO/P3HT, and ITO/AgP/P3HT:PCBM vs ITO/P3HT:PCBM), in spite of the thicknesses of the films being roughly half those of the films without AgPs. Thus, the effect of AgPs on photocurrent enhancement was verified even for P3HT and

Figure 6

P3HT:PCBM films.

Figure 6 shows IPCE profiles of the four sample films. Another noteworthy result is that in the presence of AgPs, the IPCE value increased rapidly at wavelengths of less than ~600 nm, where the plasmon band of AgPs appeared. All of these results are reasonably consistent with each other; thus, we can conclude that AgPs are effective for the enhancement of photocurrent generation in both P3HT and P3HT:PCBM systems.

4. Conclusions

We have verified that AgPs can serve as a nanomaterial for the enhancement of photocurrent signals in organic photovoltaic systems. There appear to be two factors causing the enhanced photocurrent: the enhancement of excited states by the plasmon electric field and light scattering. Also, the bottom-up fabrication and incorporation of AgPs by a wet process offer a significant improvement in the simple and large-scale fabrication of organic solar cells. Further work from this viewpoint is in progress.

References

- 1) C. W. Tang: Appl. Phys. Lett. **48** (1986) 183.
- 2) M. Hiramoto, H. Fujiwara, and M. Yokoyama: Appl. Phys. Lett. **58** (1991) 1062.
- 3) G. Yu, J. C. Hummelen, F. Wudl, and A. J. Heeger: Science, **279** (1995) 1789.
- 4) H. Hoppe and N. S. Sariciftci: J. Mater. Res. **19** (2004) 1924
- 5) F. Wudl: Acc. Chem. Res. **25** (1992) 157
- 6) F. Padinger, R. S. Rittberger, and N. S. Sariciftci: Adv. Funct. Mater. **13** (2003) 85
- 7) W. Ma, C. Yang, X. Gong, K. Lee, and A. J. Heeger: Adv. Funct. Mater **15** (2003) 85
- 8) K. Tvingstedt, N. K. Persson, O. Inganäs, A. Rahachou, and I. V. Zozoulenko: Appl. Phys. Lett. **91** (2007) 113514.
- 9) K. L. Kelly, E. Coronado, L. L. Zhao, and G. C. Schatz: J. Phys. Chem. B **107** (2003) 668.
- 10) S. Mookapat, F. J. Beck, A. Polman, and K. R. Catchpole: Appl. Phys. Lett. **95** (2009) 053115.
- 11) F. J. Haug, T. Söderström, O. Cubero, V. Terrazzoni-Daudrix, and C. Ballif: J. Appl. Phys. **104** (2008) 064509.
- 12) K. Nakayama, K. Tanabe, and H. A. Atwater: Appl. Phys. Lett. **93** (2008) 121904.
- 13) H. Nakamura, H. Yanagi, T. Kita, A. Magario, and T. Noguchi: Appl. Phys. Lett. **92** (2008) 243302.
- 14) S. D. Standridge, G. C. Schatz, and J. T. Hupp: Langmuir **25** (2009) 2596.
- 15) K. Aslan, M. Wu, J. R. Lakowicz, and C. D. Geddes: J. Am. Chem. Soc. **129** (2007) 1524.
- 16) J. R. Lakowicz, Y. Shen, S. D'Auria, J. Malicka, J. Fang, Z. Gryczynski, and I. Gryczynski: Anal. Biochem. **301** (2002) 261.
- 17) S. D. Standridge, G. C. Schatz, and J. T. Hupp: J. Am. Chem. Soc. **131** (2009) 8407.

- 18) D. M. Schaadt, B. Feng, and E. T. Yu: Appl. Phys. Lett. **86** (2005) 063106.
- 19) S. P. Sundararajan, N. K. Grady, N. Mirin, and N. J. Halas: Nano Lett. **8** (2008) 624.
- 20) S. H. Lim, W. Mar, P. Matheu, D. Derkacs, and E. T. Yu: J. Appl. Phys. **101** (2007) 104309.
- 21) R. B. Konda, R. Mundle, H. Mustafa, O. Bamiduro, A. K. Pradhan, U. N. Roy, Y. Cui, and A. Burger: Appl. Phys. Lett. **91** (2007) 191111.
- 22) M. K. Kwon, J. Y. Kim, B. H. Kim, I. K. Park, C. Y. Cho, C. C. Byeon, and S. J. Park: Adv. Mater. **20** (2008) 1253.
- 23) S. Pillai, K. R. Catchpole, T. Trupke, G. Zhang, J. Zhao, and M. A. Green: Appl. Phys. Lett. **88** (2006) 161102.
- 24) H. R. Stuart and D. G. Hall: Appl. Phys. Lett. **73** (1998) 3815.
- 25) S. Collin, F. Pardo, and J. L. Pelouard: Appl. Phys. Lett. **83** (2003) 1521.
- 26) L. Tang, D. A. B. Miller, A. K. Okay, J. A. Matteo, Y. Yuen, K. C. Saraswat, and L. Hesselink: Opt. Lett. **31** (2006) 1519.
- 27) D. Derkacs, S. H. Lim, P. Matheu, W. Mar, and E. T. Yu: Appl. Phys. Lett. **89** (2006) 093103.
- 28) S. Pillai, K. R. Catchpole, T. Trupke, and M. A. Green: J. Appl. Phys. **101** (2007) 093105.
- 29) H. R. Stuart and D. G. Hall: Appl. Phys. Lett. **69** (1996) 2327.
- 30) C. Hägglund, M. Zäch, G. Petersson, and B. Kasemo: Appl. Phys. Lett. **92** (2008) 053110.
- 31) T. Arakawa, T. Akiyama, and S. Yamada: Trans. Mater. Res. Soc. Jpn. **33** (2008) 185.

- 32) T. Arakawa, T. Munaoka, T. Akiyama, and S. Yamada: J. Phys. Chem. C **113** (2009) 11830.
- 33) P. J. G. Goulet, D. S. dos Santos, R. A. Alvarez-Puebla, O. N. Oliveira, and J. R. F. Aroca: Langmuir **21** (2005) 5576.
- 34) P. Vanlaeke, A. Swinnen, I. Haeldermans, G. Vanhoyland, T. Aernouts, D. Cheyns, C. Deibel, J. D' Haen, P. Heremans, J. Poortmans, and J. V. Manca: Sol. Energy Mater. Sol. Cells **90** (2006) 2150.
- 35) C. Y. Liu, Z. C. Holman, and U. R. Kortshagen: Nano Lett. **9** (2009) 449.
- 36) S. Cook, R. Katoh and A. Furube: J. Phys. Chem. C **113** (2009) 2547.
- 37) S. van Bavel, E. Sourty, G. de With, K. Frolic, and J. Loos: Macromolecules **42** (2009) 7396.

Figure Captions

Fig. 1 Molecular structures of P3HT and PCBM.

Fig. 2 Schematic illustration of the fabrication of P3HT and P3HT:PCBM films with or without AgPs: (a) ITO/AgP/P3HT; (b) ITO/AgP/P3HT:PCBM; (c) ITO/P3HT; (d) ITO/P3HT:PCBM.

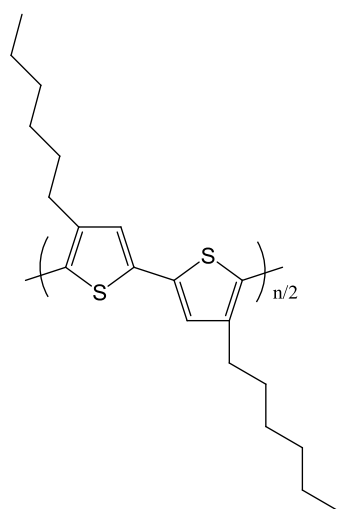
Fig. 3 Transmission absorption spectra of (a) ITO/AgP/P3HT; (b) ITO/AgP/P3HT:PCBM; (c) ITO/P3HT; (d) ITO/P3HT:PCBM.

.

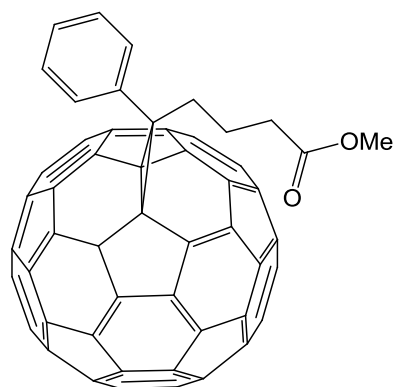
Fig. 4 AFM images of ITO/AgP of ITO/AgP/P3HT (a) and ITO/AgP/P3HT:PCBM (b) before spin coating.

Fig. 5 Emission spectra of (a) ITO/AgP/P3HT; (b) ITO/AgP/P3HT:PCBM; (c) ITO/P3HT; (d) ITO/P3HT:PCBM.

Fig. 6 Incident photon-to-current conversion efficiencies (IPCE%) spectra of (a) ITO/AgP/P3HT; (b) ITO/AgP/P3HT:PCBM; (c) ITO/P3HT; (d) ITO/P3HT:PCBM.



P3HT



PCBM

Fig. 1 You et al.

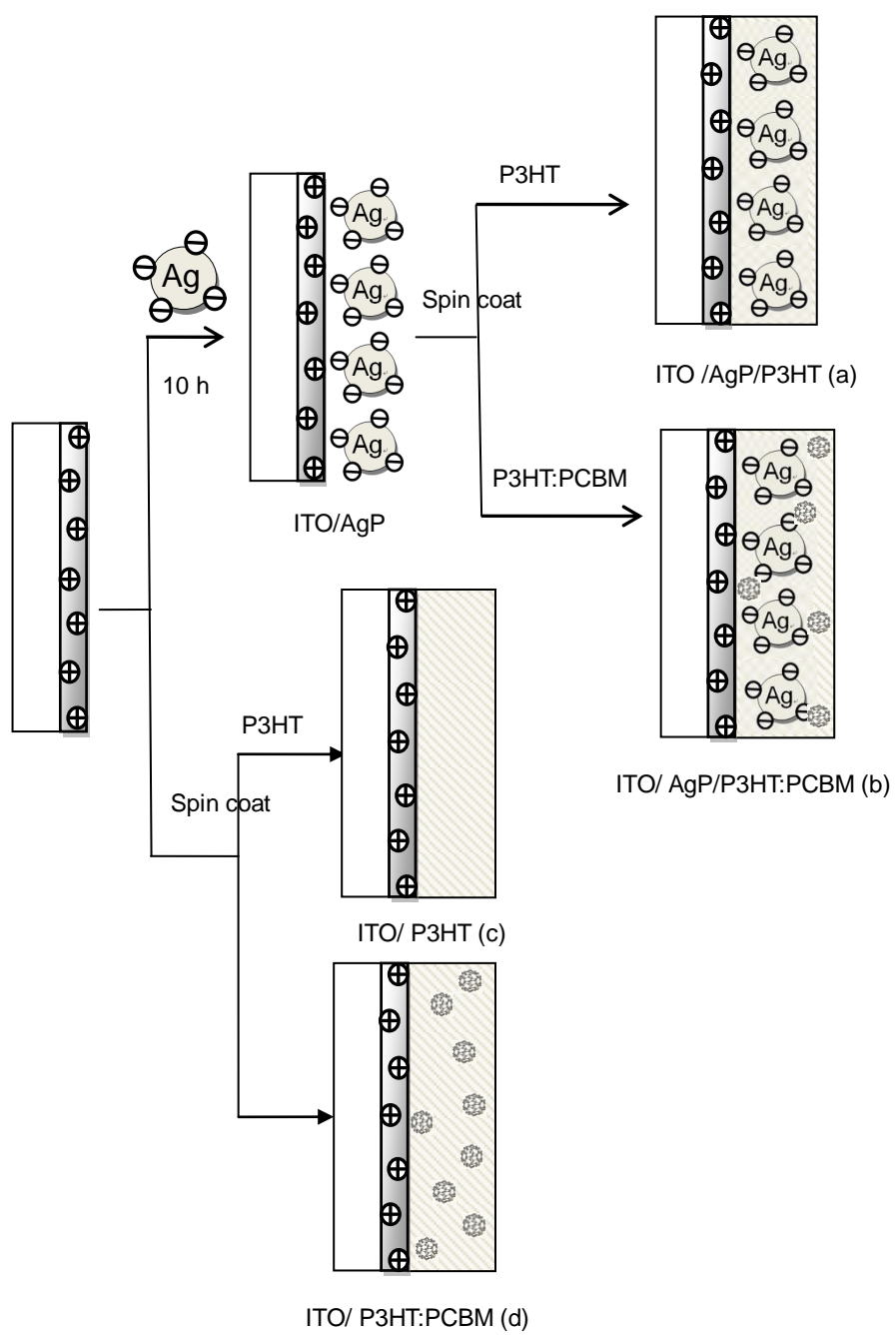


Fig. 2 You et al.

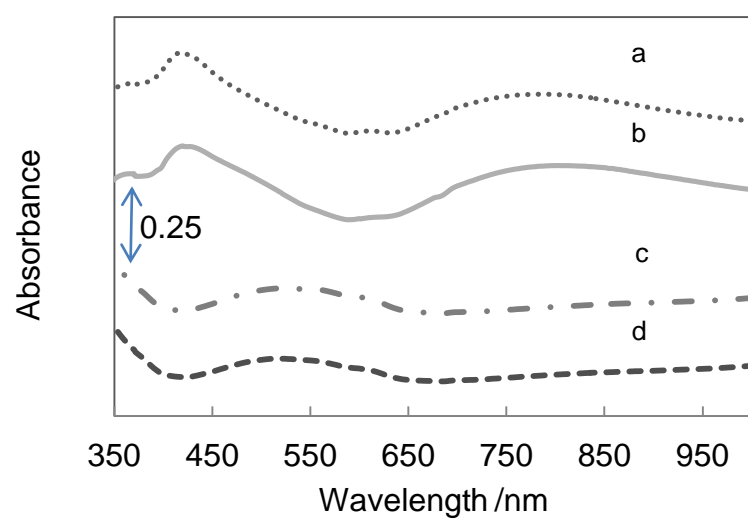


Fig. 3 You et al.

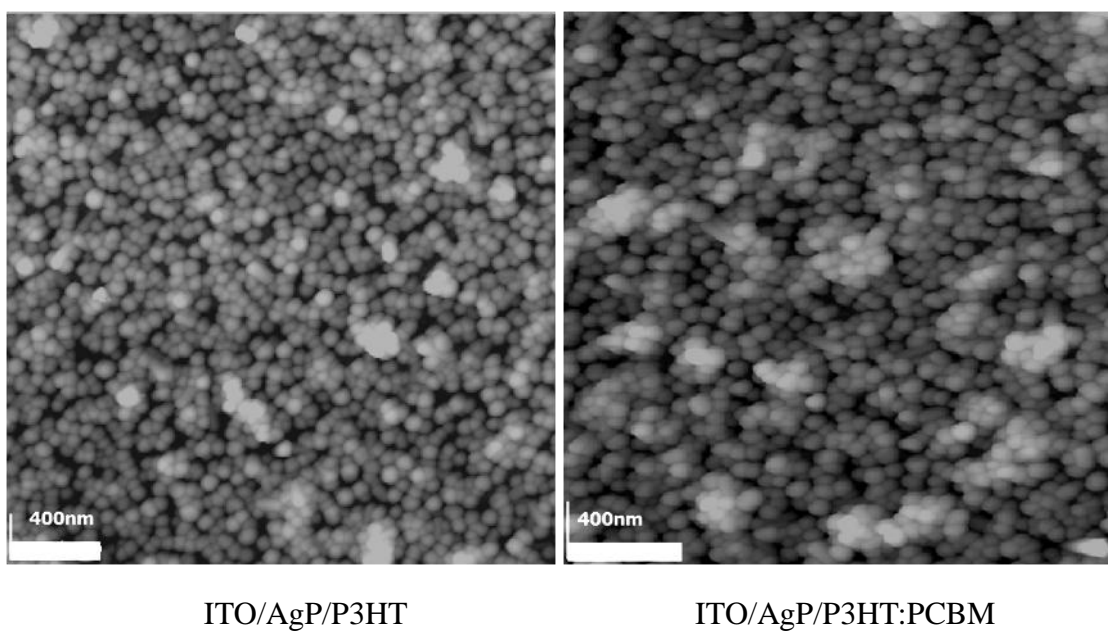


Fig. 4 You et al.

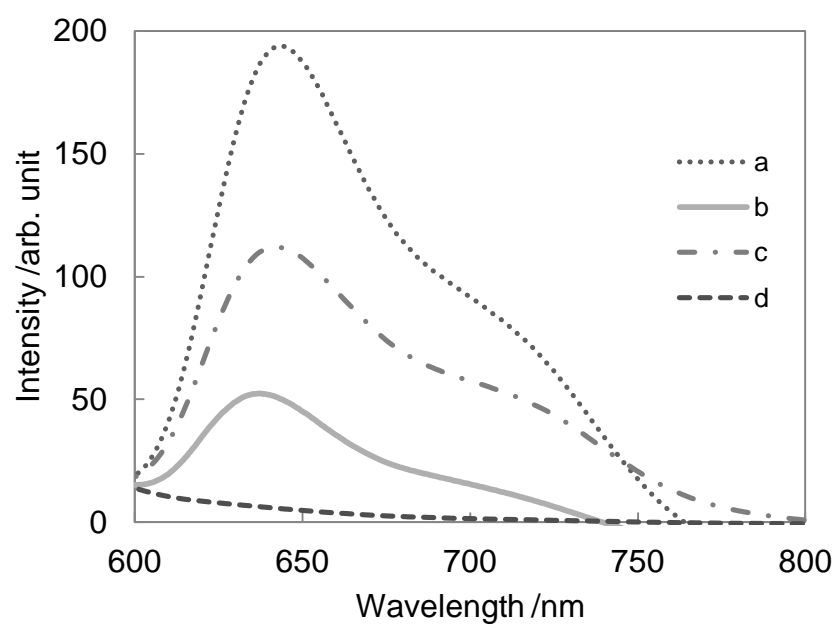


Fig. 5 You et al.

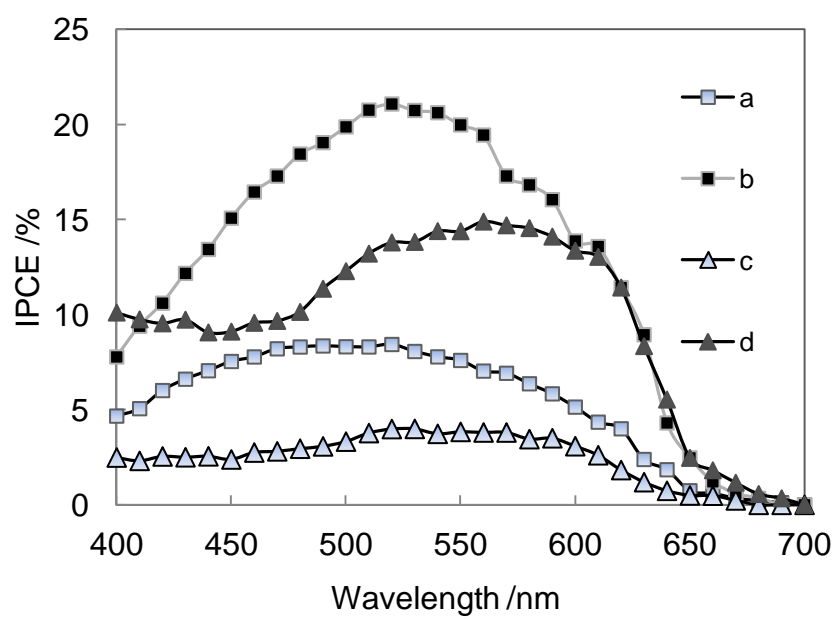
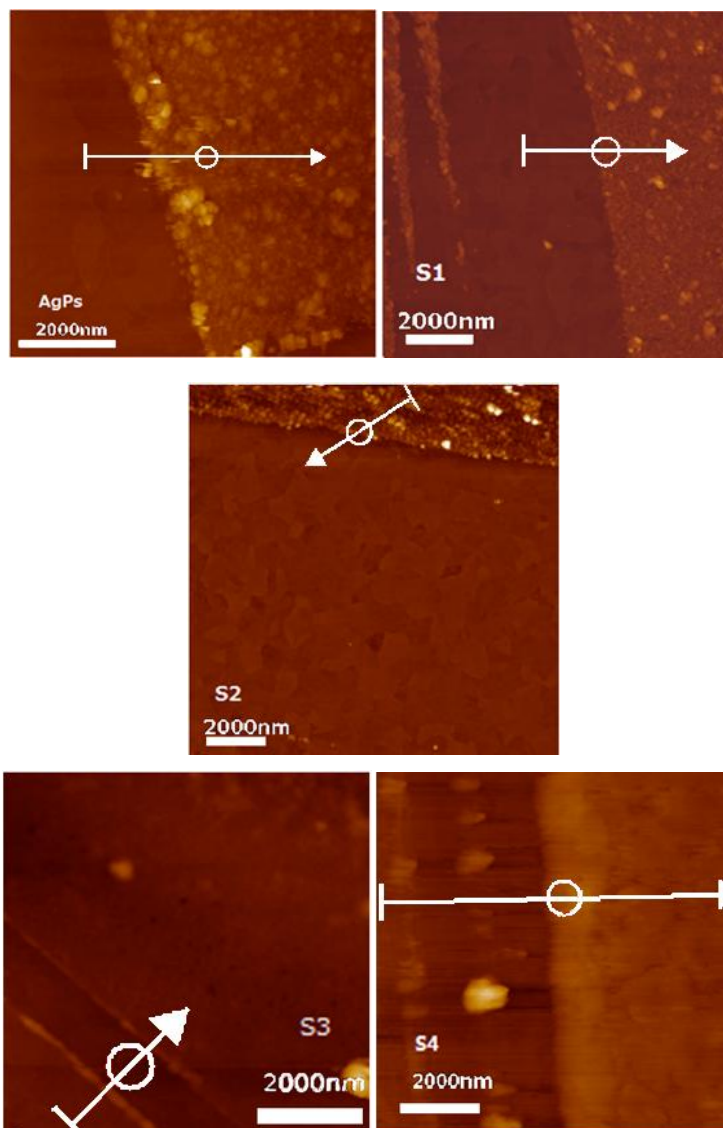


Fig. 6 You et al.

Supporting Information

We have just removed the film region of each sample, than the height data were acquired.



Thicknesses of films are listed in following table:

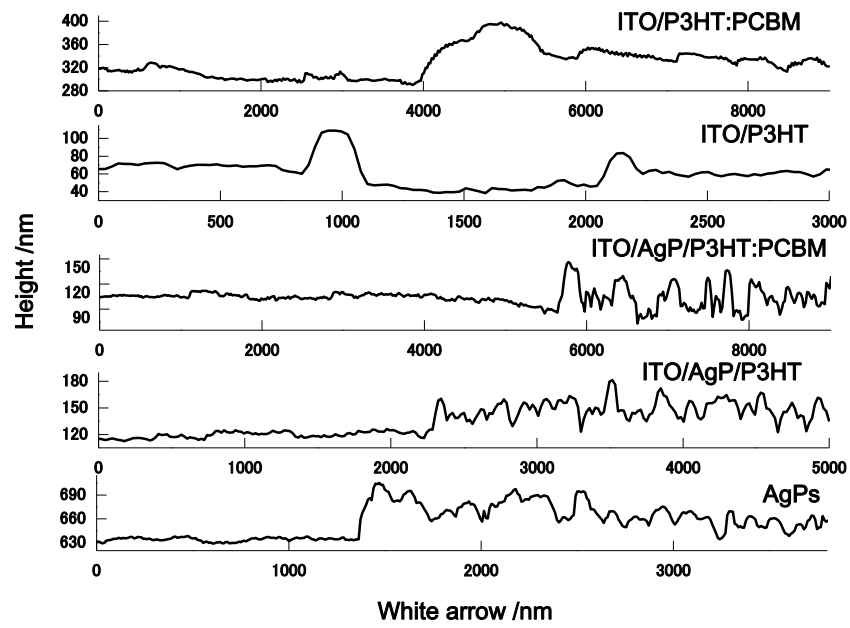


Table 1. Thickness of P3HT or P3HT:PCBM layer.

	ITO/AgP/P3HT	ITO/AgP/P3HT:PCBM	ITO/P3HT	ITO/P3HT:PCBM
Thickness /nm	15 ± 5	21 ± 3	25 ± 5	33 ± 6